Oxide-apertured VCSEL with short period superlattice

Lin Li (李 林), Jingchang Zhong (钟景昌), Yongming Zhang (张永明), Wei Su (苏 伟), Yingjie Zhao (赵英杰), Changling Yan (晏长岭), Yongqin Hao (郝永琴), and Xiaoguang Jiang (姜晓光)

National Key Lab of High Power Semiconductor Lasers, Changchun University of Science and Technology, Changchun 130022

Received February 9, 2004

Novel distributed Bragg reflectors (DBRs) with 4.5 pairs of GaAs/AlAs short period superlattice (SPS) used in oxide-apertured vertical-cavity surface-emitting lasers (VCSELs) were designed. The structure of a 22-period $Al_{0.9}Ga_{0.1}As$ (69.5 nm)/4.5-pair [GaAs (10 nm)-AlAs (1.9 nm)] DBR was grown on an n^+ GaAs substrate (100) 2° off toward ⟨111⟩A by molecular beam epitaxy. The emitting wavelength was 850 nm with low threshold current of about 2 mA, corresponding to the threshold current density of 2 kA/cm^2. The maximum output power was more than 1 mW. The VCSEL device temperature was increased by heating ambient temperature from 20 to 100 °C and the threshold current increased slowly with the increase of temperature.

OCIS codes: 140.5960, 140.6810, 230.1480, 250.7260.

The distributed Bragg reflectors (DBRs) determine some important optical and electrical characteristics of vertical cavity surface emitting lasers (VCSELs), and it is desirable to use semiconductor DBRs to allow injection current into the structure through the reflectors[1]. The semiconductor DBRs consist of two kinds of semiconductor materials, so we may call it semiconductor/semiconductor DBRs. The semiconductor materials with large differences in refractive indices, however, have large band-gap differences, that cause high electrical resistance and excess power consumption. Therefore, many kinds of modified heterointerface structures were designed so as to reduce the electrical resistance of semiconductor DBRs[2], which complicate their design and fabrication and may also deteriorate the characteristics of VCSELs.

Taking into account the tunneling effect of the superlattices, GaAs in the DBR was replaced with a superlattice [GaAs-AlAs], and a novel $Al_{0.9}Ga_{0.1}As$-[GaAs-AlAs] semiconductor/superlattice DBR was proposed. The tunneling effect of the superlattice with quantum size increases the tunneling current in the VCSEL that is an equivalent for the decrease of electrical resistance of the device. A numerical simulation of the design of a novel DBR with short period superlattices (SPSs) was reported[3]. According to the simulative results, a novel DBR with GaAs/AlAs SPSs was designed.

The epitaxial layers were grown on an n^+ GaAs substrate (100) 2° off towards ⟨111⟩A by molecular beam epitaxy. The structure of a 1-period $Al_{0.9}Ga_{0.1}As$-[GaAs-AlAs] superlattice Bragg mirror is shown in Fig. 1. The thickness of $Al_{0.9}Ga_{0.1}As$ layer is 69.5 nm and the superlattice consists of 4.5 pairs of GaAs (10 nm)-AlAs (1.9 nm). The VCSEL was designed for 850-nm wavelength. 34-period $Al_{0.9}Ga_{0.1}As$ (69.5 nm)/4.5-pair [GaAs (10 nm)-AlAs (1.9 nm)] n-type (Si-doped, $(1-3)\times10^{18}/cm^3$) mirrors, three-quantum-well active region, and 22-period $Al_{0.9}Ga_{0.1}As$ (69.5 nm)/4.5-pair [GaAs (10 nm)-AlAs (1.9 nm)] p-type (Be-doped, $(3-5)\times10^{18}/cm^3$) mirrors were grown. In addition, a 35-nm layer of $Al_{0.98}Ga_{0.02}As$ was inserted in the mirrors for selective lateral oxidation.

The fabrication process began with defining Ti/Pt/Au ring contacts with the size of 30 μm, then patterned photoresist was used as etch masks for $BCl_3/Cl_2/SiCl_4$ reactive ion etching (RIE). When the high-aluminum content oxidation layer was exposed, the sample was oxidized at 460 °C under N_2 gas bubbled through de-ionized water at 90 °C, the $Al_{0.98}Ga_{0.02}As$ layer was oxidized for 10 minutes to form a 10-μm current aperture. After lateral oxidation, 400-nm-thick SiN_x was deposited in a plasma-enchanced chemical vapor deposition (PECVD) system for electrical isolation. Finally, the SiN_x film was removed from the top of the pillars in CF_4 plasma.

The reflection spectrum of the VCSEL was taken with the WDH3 wide-wavelength scanning spectrometer, as shown in Fig. 2, which shows that the central wavelength is at about 850 nm, and the reflection bandwidth is about 70 nm.

After device fabrication, we tested VCSEL characteristics. Figure 3 shows the VCSEL's emission spectrum, which confirms single mode operation with the peak at the wavelength of about 850 nm. The spectral linewidth

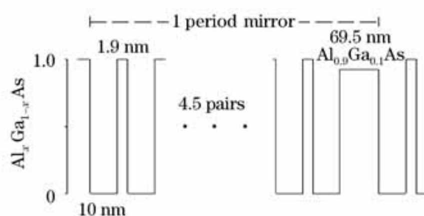

Fig. 1. The schematic diagram of one period of DBR structure.

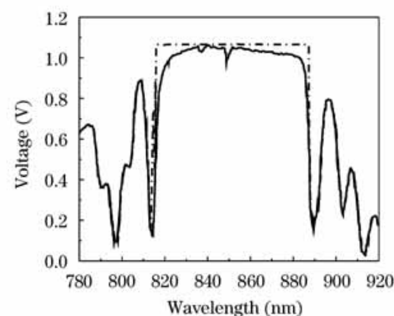

Fig. 2. The theoretical dashed curve and measured solid curve reflection spectra.

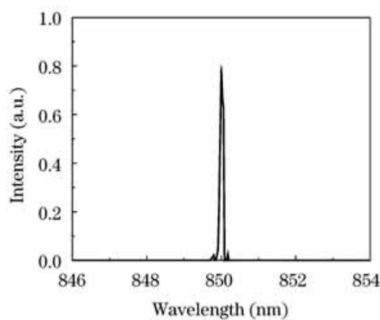

Fig. 3. The VCSEL's emission spectrum.

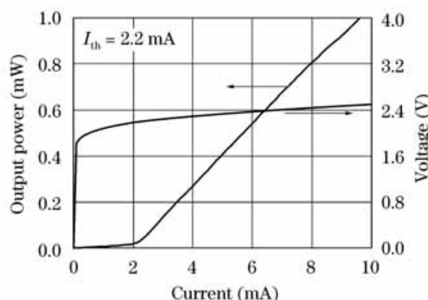

Fig. 4. The light-current-voltage characteristics of the VCSEL, the threshold current is about 2 mA.

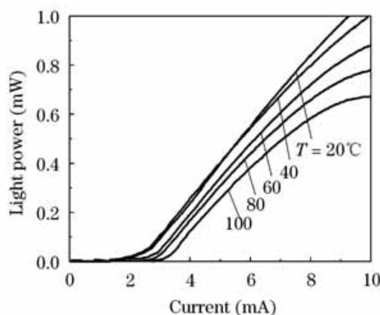

Fig. 5. VCSEL output power versus current (P-I) measured characteristics under different temperatures.

in this graph was limited by the spectrometer to 0.1 nm.

Figure 4 shows the typical light output power-current (P-I) and voltage-current (V-I) characteristics at room temperature (20 °C). The threshold current was 2 mA, which corresponded to the threshold current density of 2 kA/cm^2.

Figure 5 shows the temperature dependence of output power characteristics under ambient temperature from 20 to 100 °C. The threshold current increases slowly with the increase of temperature. The temperature characteristics under both continuous wave (CW) and pulsed operation for several VCSELs were measured. The devices were tested with a pulse width of 1 μs and a repetition rate of 2 kHz in order to avoid thermal effects. The current was fixed to provide an output power of 1 mW at room temperature.

As shown in Fig. 5, temperature affects the P-I characteristics and the effect of temperature increase on the threshold current $I_{\rm th}(T)$ is often described by a characteristic temperature (T_0). VCSEL exhibits quite different temperature dependences. We obtain a function T_0 which decreases from 220 K at room temperature to 200 K at 100 °C. VCSEL performance generally degrades with increasing temperature.

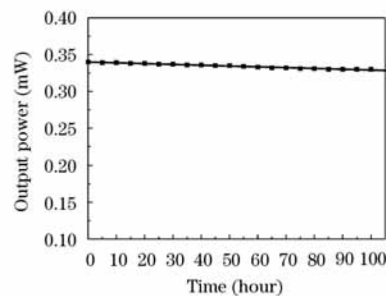

Fig. 6. Output power versus time under the conditions of 60 °C, 5 mA.

The drive current not only affects degradation rate directly, but also significantly affects junction heating due to the high thermal resistance of VCSEL. For a VCSEL with a 10-μm-diameter oxide aperture, 5 mA is perhaps a typical average bias current at 70 °C, but the current up to 7 mA is acceptable[4]. The thermal resistance R[5] of VCSEL was calculated, the thermal resistance is estimated to be approximately 16 K/mW. Figure 6 shows the reliability of VCSEL devices. The reliability test condition were set to 60 °C, 5 mA. During 100 hours, no obvious failures were observed, which implies that the devices work stably with a long lifetime.

The essential improvements for the oxide-apertured VCSEL in this work are focused on the following two points. Firstly, we decrease the series resistance of the VCSEL. Secondly, the oxide confinement technique by forming an oxide surface barrier reduces defects and optical absorption in the active region. The oxide-apertured technique is worth using because of its better confinements for both beam and current, easier processing, and lower cost. The fact that the device's threshold current in CW and pulse operation slightly depends on ambient temperature means that the VCSEL's characteristic temperature is higher.

In conclusion, a novel DBR with 4.5-pair GaAs/AlAs SPSs was designed. The threshold current increases slowly with the increase of temperature. Comparing the conventional VCSEL with semiconductor/semiconductor DBRs, the oxide-apertured VCSEL with SPSs improves the performance. The replacement of semiconductor materials with superlattices plays a key role in this case.

This work was supported by the National Natural Science Foundation of China under Grant No. 60306004. L. Li's e-mail address is lilinciom@sina.com.cn.

References

1. W. W. Chow, K. D. Choquette, M. H. Crawford, K. L. Lear, and G. R. Hadley, IEEE J. Quantum Electron. **33,** 1810 (1997).
2. S. A. Chalmers, K. L. Lear, and K. P. Killeen, Appl. Phys. Lett. **62,** 1585 (1993).
3. W. Su, J. C. Zhong, W. L. Liu, Y.-K. Su, S.-J. Chang, H.-C. Yu, L. W. Ji, L. Li, and Y. J. Zhao, Chin. Opt. Lett. **1,** 674 (2003).
4. R. W. Herrick, Proc. SPIE **4649,** 130 (2002).
5. T. Kondo, M. Arai, M. Azuchi, T. Uchida, A. Matsutani, T. Miyamoto, and F. Koyama, Jpn. J. Appl. Phys. **41,** L562 (2002).